Ultrasonic Seismic Wave Elastic Moduli, λρ-μρ space and Attenuation: Petrophysical Models and Work Flows for Better Subsurface Imaging, and Tracking of Sequestered CO_2.

William Harbert, Zan Wang, Robert Dilmore, Igor Haljasmaa, Dustin Crandall, Yee Soong,

Research & Innovation Center

NATIONAL ENERGY TECHNOLOGY LABORATORY

Goal:

Parameters related to seismic and ultrasonic elastic waves traveling through a porous rock material with compliant pores, cracks and isometric pores, and pore filling fluids are subject to variations that are dependent on petrophysical properties. Experiments simulating subsurface conditions were performed in the Geomechanics and Flow Laboratory at the National Energy Technology Laboratory (NETL) of the United States Department of Energy (DOE) with varied pore-filling fluids, effective pressures (0.01 to 50 MPa), and temperatures (21° to 80° C). Ultrasonic compressive and shear wave V_P, V_{S1} and V_{S2} velocities were measured using a New England Research (NER) Autolab 1500 device, allowing calculation of the dynamic moduli parameters. Using an aluminum reference core and the ultrasonic waveform data collected, we employed the spectral ratio method to estimate the quality factor for the P ultrasonic seismic phase. The quality factor (Q_p) is a dimensionless value that represents the attenuation of a seismic wave as it travels through a rock. Carbonate samples were tested dry, using atmospheric gas as the pore phase, as well as saturated with deionized water, oil, and supercritical CO_2. Our research indicates framework composition, porosity, heterogeneities, temperature, pressure and pore filling fluids are physical controls on wave attenuation and shifts trends in the Young's Modulus-Poisson's Ratio and λρ-μρ cross plot spaces. The effects of temperature and pressure on elastic attenuation and λρ-μρ are less significant than porosity and rock heterogeneities. The presence of fluids causes a distinct shift in λρ values, an observation which could provide insight into subsurface exploration using amplitude variation with offset (AVO) classification.

Approach

Wave velocity and rock moduli data was collected for 20 separate rock cores. The elastic moduli (including the Lamé parameters) are ratios of applied stresses and the resulting strain in linear elastic materials. These moduli indicate how the rock responds to applied stress, including those related to the propagation of compressional and shear waves in the subsurface. Knowledge of these parameters allows complete understanding the stress and strain relations of a material. After both P and S wave velocities were recorded at various effective pressures, the dynamic elastic moduli were calculated using the standard equations:

- $V_p = \sqrt{\frac{\lambda+2\mu}{\rho}}$
- $V_s = \sqrt{\frac{\mu}{\rho}}$

Both the P and S-wave acoustic impedances are directly related to the Lamé parameters and in particular λρ and μρ. The relationship between elastic moduli and acoustic impedance is given by the following relationships (Goodway, 2001).

- $I_p^2 = \lambda\rho + 2\mu\rho$ and $I_s^2 = \mu\rho$

The petrophysical model we used follows that proposed Zimmerman et al., (1986), Eberhart-Phillips et al. (1989) as extended and modified by Shapiro et al., (2005) and Shapiro and Kaselow (2005). Zimmerman et al., (1986) and Eberhart-Pphillips et al., (1989), the velocity as a function of effective pressure ($V(_{Peff})$) was shown to be represented as:

- $V(P_{eff}) = A + BP_{eff} - Ce^{(-P_{eff}D)}$

Where A, B, C, and D represent calculated numerical fitting parameters. In the theoretically derived equations, (Mavko et al., 1998, 2009; Shapiro et al., 2005; Shapiro and Kaselow 2005) this relationship was derived and K_{dry} and μ_{dry} elastic characteristics as a function of P_{eff}, central to Gassman-Biot fluid substitution modeling. We used equations of this form:

- $K_{Dry}(P_{eff}) = K_{DryS}\left[1 + \theta_S\left(\frac{1}{K_{DryS}} - \frac{1}{K_0}\right)P_{eff} - \vartheta_{c0}\theta_c e^{-(-\theta_c P_{eff}/K_{DryS})}\right]$
- $\mu_{Dry}(P_{eff}) = \mu_{DryS}\left[1 + \theta_{S\mu}\left(\frac{1}{K_{DryS}} - \frac{1}{K_0}\right)P_{eff} - \vartheta_{c0}\theta_c e^{-(-\theta_c P_{eff}/K_{DryS})}\right]$

Details of this approach(Gassmann 1951, McKenna et al. 2003) can be found in Mur (2008) and Delaney et al., (2017)

- $K_{sat} = K_{dry} + \frac{(1-\frac{K_{dry}}{K_0})^2}{\frac{\phi}{K_{fluid}}+\frac{1-\phi}{K_0}-\frac{K_0}{K_0^2}}$

along with a bulk density summation where ρ_{fluid} is the density at a given pressure and $\rho_{mineral}$ is the mineral density (assumed constant

- $\rho_{bulk}(P_{eff}) = (1-\phi)\rho_{mineral} + \phi\rho_{fluid}(P_{eff})$

to calculate pressure dependent P and S-wave velocities:

- $V_P(P_{eff}) = \sqrt{\frac{(K_{sat}+(4/3)\mu_{sat})}{\rho_{bulk}}}$
- $V_S(P_{eff}) = \sqrt{\frac{\mu_{sat}}{\rho_{bulk}}}$

Using pressure dependent elastic parameters, modeled results can be compared with experimental results. Cross plots of density independent Young's modulus (E), Shear modulus (μ), Poisson's ratio (v), and Bulk modulus (K),

- $E = 3K(1-2v)$
- $\mu = \frac{3K(1-2v)}{2(1+v)}$
- $v = \frac{E}{2\mu} - 1$
- $K = \frac{E}{3(1-2v)}$

can be used to further emphasize and understand stress dependence of the material.

To calculate the quality factor Q from ultrasonic measurements we employed the spectral ratio method. This method compares the input wave spectrum to the output wave spectrum. To derive the spectral ratio formulation for Q estimation we take the log using

- $ln\left[\frac{A_{ref}}{A_{rock}}\right] = ln\left[\frac{G_{ref}}{G_{rock}}e^{-xf[\gamma_{rock}-\gamma_{ref}]}\right] = f\gamma_{rock}x + \ln\left(\frac{G_{ref}}{G_{rock}}\right)$

(A) Project workflow diagram highlighting the experiments performed on each core and applications. (B) Core measurement workflow showing steps completed to determine the relevant dynamic parameters reviewed in this poster.

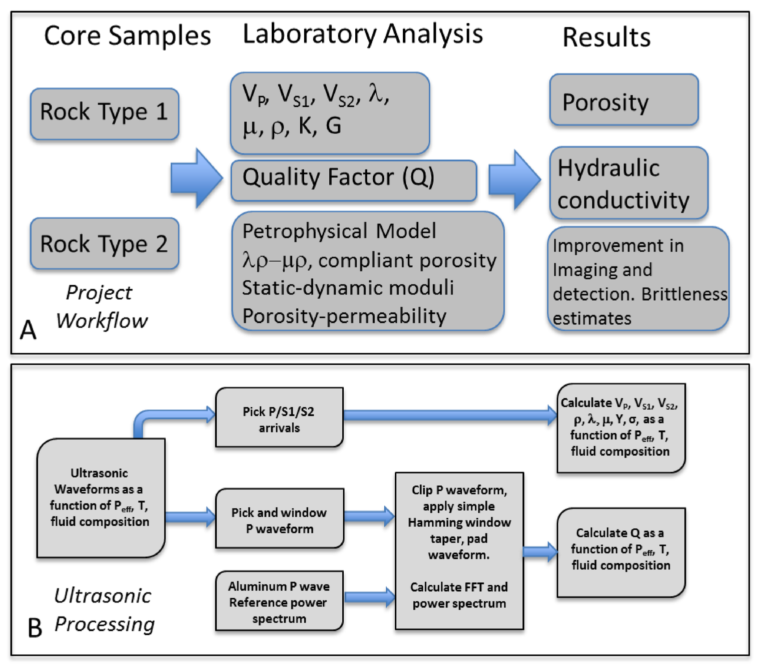

- Ultrasonic velocity experiments were performed at the National Energy Technology Laboratory under in situ pressure/temperature conditions for various pore fluids.

Left: NER Autolab 1500 Center: Sonic velocity core holder assembly Right: Resistivity heads with limestone core.

COMPLIANT POROSITY

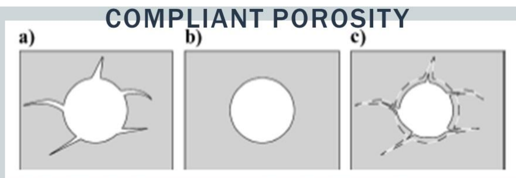

Idealized sketch of pore space. (a) In the unloaded state, the pore space consists of stiff pores and compliant pores, in contrast to (b) the reference state, where the pore space consists only of stiff pores. (c) In the loaded case, both stiff and compliant pores are deformed by an applied load. (Shapiro 2005)

- Velocity increases dramatically over the effective pressure range 0.1 to 15 Mpa. Increase is attributed to increasing bulk modulus. Bulk modulus increases because of closing of compliant porosity:
  - Pores with high aspect ratio close more easily under pressure
  - Complex cracks on the edge of large pores, although not separate pores, will close first.

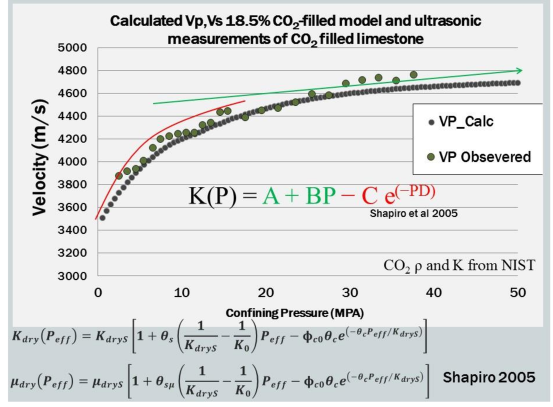

$K_{dry}(P_{eff}) = K_{dryS}\left[1 + \theta_s\left(\frac{1}{K_{dryS}} - \frac{1}{K_0}\right)P_{eff} - \phi_{c0}\theta_c e^{(-\theta_c P_{eff}/K_{dryS})}\right]$

$\mu_{dry}(P_{eff}) = \mu_{dryS}\left[1 + \theta_{s\mu}\left(\frac{1}{K_{dryS}} - \frac{1}{K_0}\right)P_{eff} - \phi_{c0}\theta_c e^{(-\theta_c P_{eff}/K_{dryS})}\right]$ Shapiro 2005

Laboratory measurements showing consistent effect of pore filling phase in this attribute space

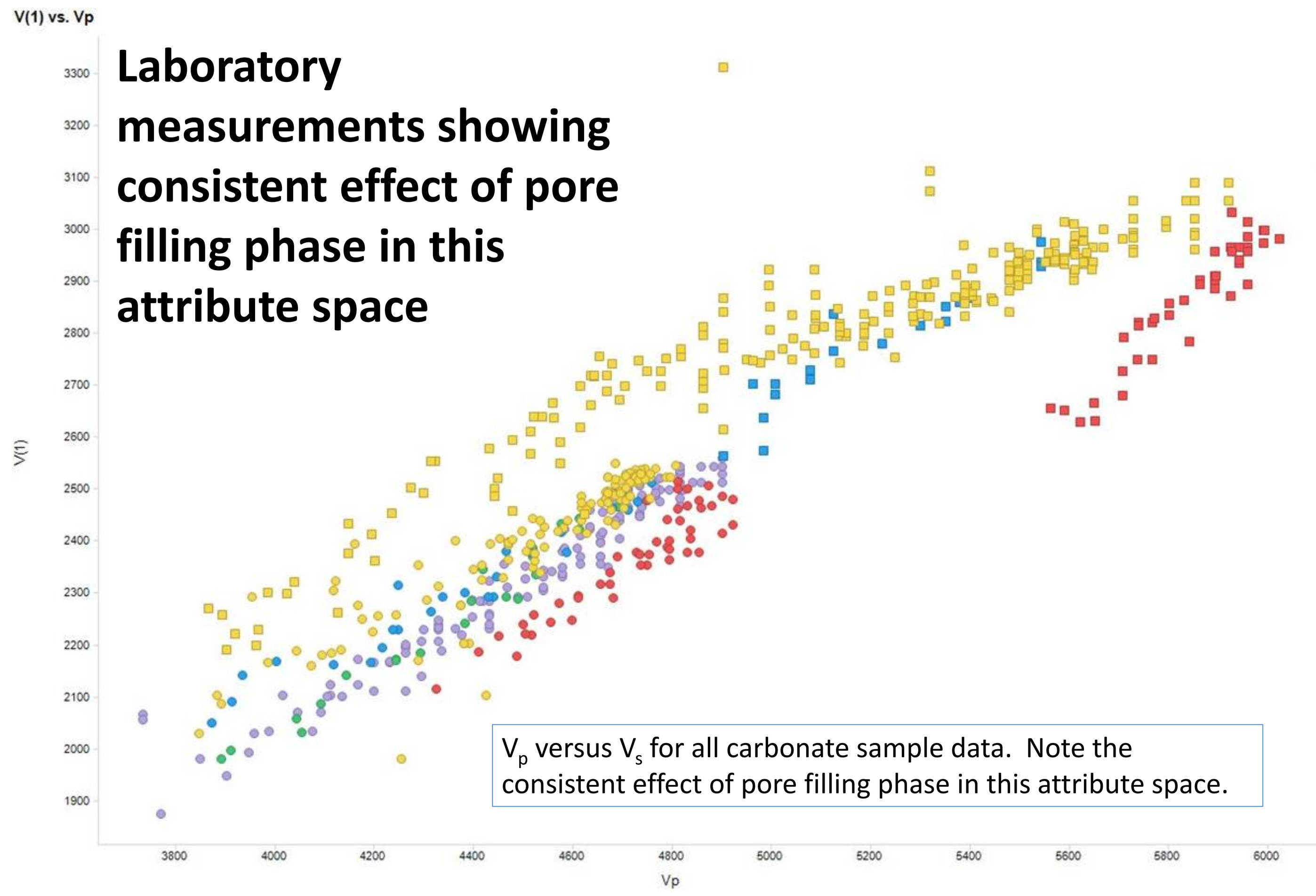

V_p versus V_s for all carbonate sample data. Note the consistent effect of pore filling phase in this attribute space.

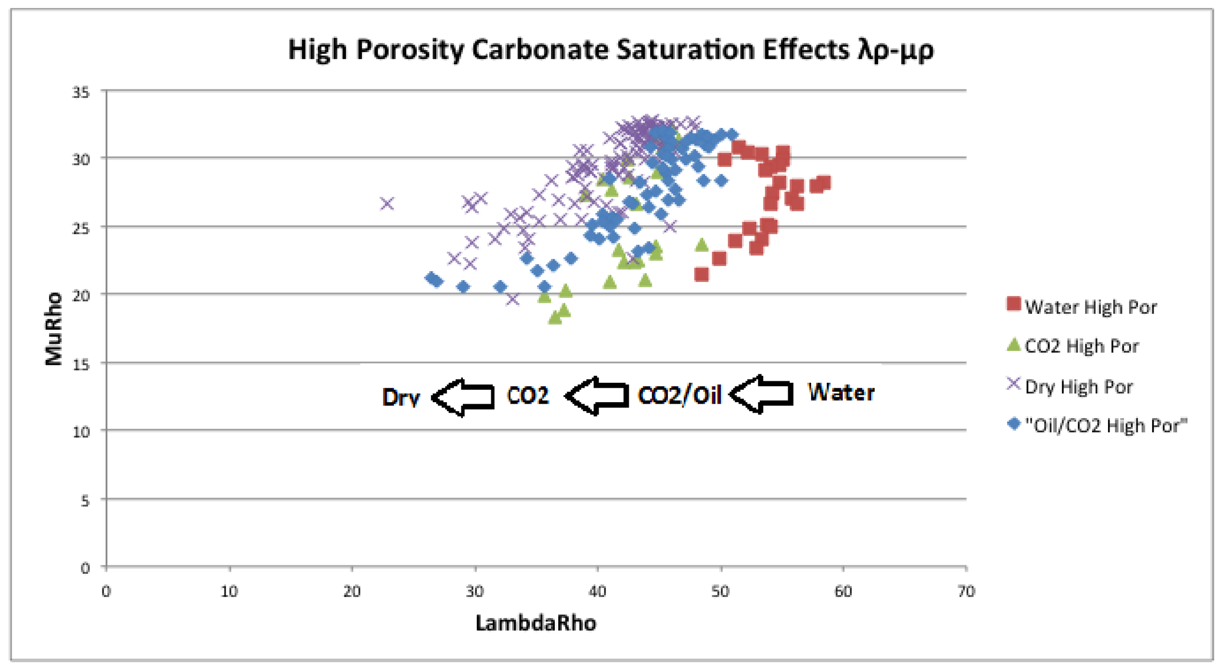

A. λρ versus μρ moduli for different pore filling phases measured at different effective pressures using the higher porosity carbonate sample.

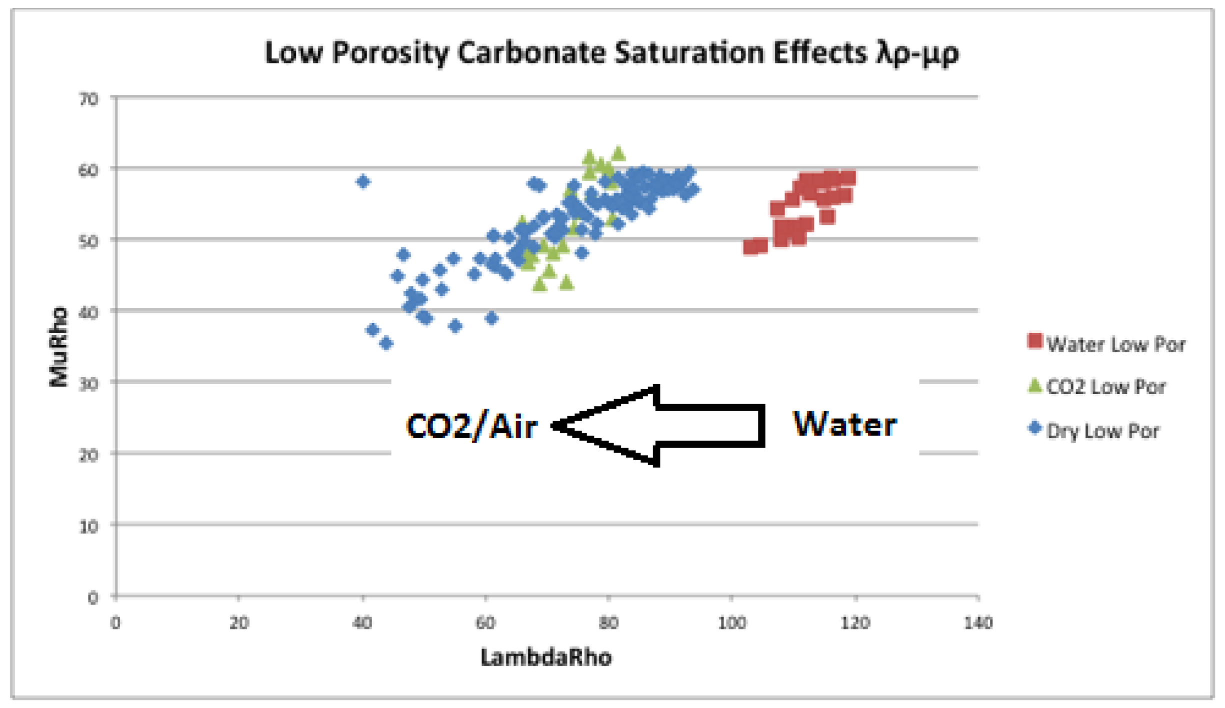

B. λρ versus μρ moduli for different pore filling phases measured at different effective pressures using the lower porosity carbonate sample.

EFFECTS OF FLUID SATURATION HIGH POROSITY CARBONATE

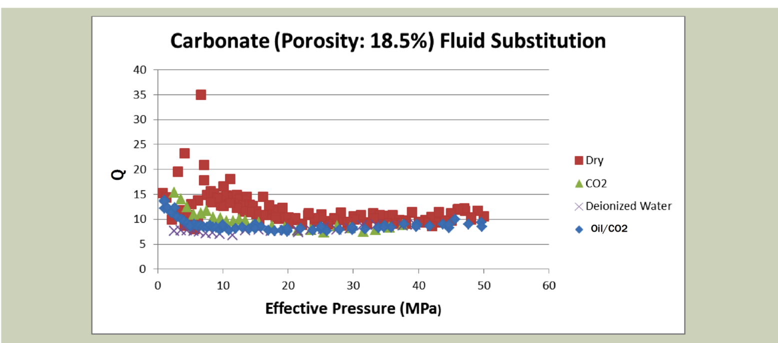

EFFECTS OF FLUID SATURATION LOW POROSITY CARBONATE

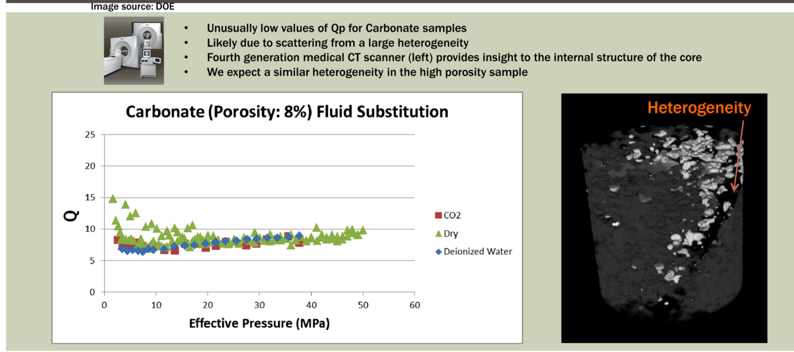

Rhyolite Samples

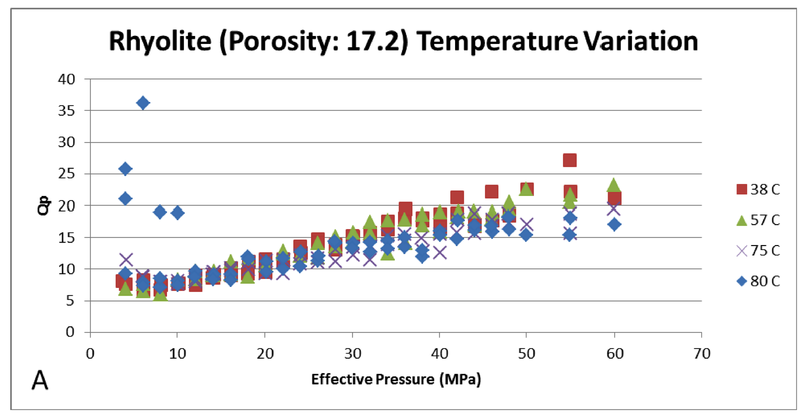

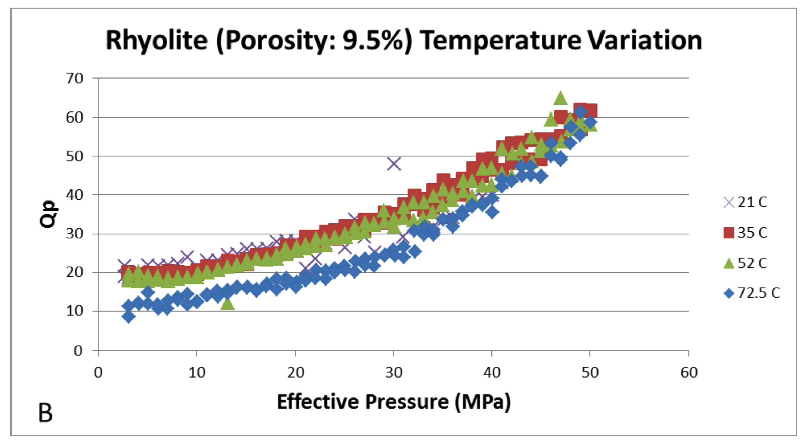

T(Above) he higher porosity core displays a significantly lower value of Q. That is to say that it seems Q is inversely proportional to porosity. These observations are consistent with those of our carbonate cores. We also note that the relationship between seismic wave attenuation and effective pressure is consistent with prior studies where Q is directly proportional to pressure (Winkler and Nur 1979; Prasad and Meissner 1992; Windler and Murphy 1995). This relationship between pressure and Q is primarily due to the effects of compliant pores closing with increasing pressure (Johnston et al. 1979). Q is also weakly dependent on sample temperature. In order to better examine the relationship between the quality factor and the temperature of the core, we plot Q_p vs. Temperature for various different effective pressures.

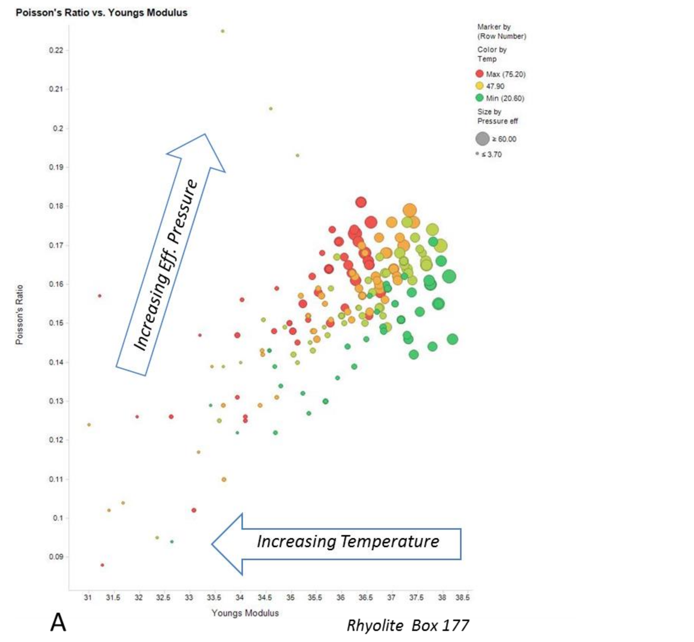

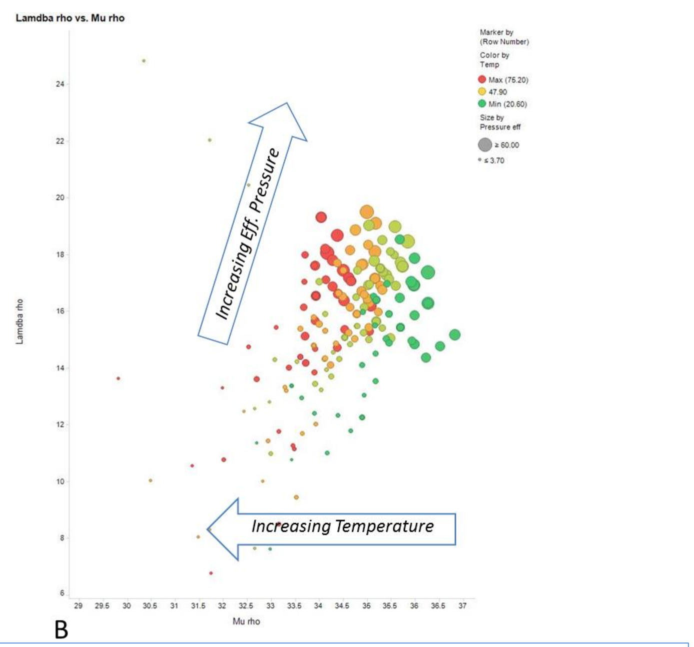

A) Interpretation Young's modulus versus Poisson's ratio and B) and B) interpretation of λρ versus μρ moduli for the two rhyolite core data measured at different temperatures.

Conclusions

- Q is directly proportional to effective pressure in our rhyolite samples
- We observe effects of core anisotropy on Q, however this is not apparent in higher porosity samples. Increasing effective pressure seems to decrease the effects of anisotropy
- Q is inversely proportional to temperature, however this does not hold true for higher porosity samples.
- Q is highly dependent on the rock porosity. Higher porosity samples display significantly lower values of Q
- Our experiments regarding Q with respect to fluid saturation are inconclusive as due to scattering in our carbonate samples. Wave scattering due to heterogeneities is dominant
- Although we observe lower μρ values, trends in our model strongly agree with the model proposed workers interpreting AVO trends in LMR space.
- μρ is proportional to temperature. λρ is temperature independent
- λρ-μρ is extremely dependent on porosity. Higher porosity results in lower values for both λρ and μρ
- Fluid saturation consistently shifts the value of λρ

The most influential physical changes affecting λρ-μρ are lithology, porosity, and fluid saturation. In terms of fluid saturation, our observations confirm Hoffe, Perez, and Goodway's model (Hoffe, Perez et al. 2008). Examination of fluid saturation in carbonate cores indicates that the introduction of pore-filling fluids shifts λρ and has little effect on μρ. We observe the shift in λρ to increase with these following sets of fluids, air, $scCO_2$, $scCO_2$/Oil and water. Our measurements expand upon Hoffe, Perez, and Goodway model (2012) by including $scCO_2$ as well as an oil/$scCO_2$ mix into the fluid trend models in order to differentiate $scCO_2$ from other pore filling phases for the purpose of carbon storage and EOR monitoring.

We have found that Q_p is inversely proportional to rock porosity and is weakly dependent on temperature. We were able to extrapolate our results to determine a relationship describing ultrasonic velocity and Q_p as a function of both temperature and effective pressure. Further experimentation is required to assess the relationship between Q_p and pore-filling fluids. However, carbonate experiments suggest that scattering effects arising heterogeneities was an important core characteristic with respect to the attenuation of seismic waves. Finally for our two carbonate cores we observed a dependence of Q_p on vertical azimuth core orientation leading us to conclude that anisotropy effects are important in the attenuation of waves in these samples.

Our thanks for including this work in poster presentation to the NRAP technical team!

Select References

•Delaney, D., Purcell, C., Mur, A., Haljasmaa, I., Soong, Y., Crandall, D., and Harbert, W., 2017, Dynamic Modulia and Attenuation: Rhyolite and Carbonate Examples, The Leading Edge (revision submitted and in review).
•Eberhart-Phillips, D., Han, D. H., and Zoback, M. D., (1989), "Empirical relationships among seismic velocity, effective pressure, porosity and clay content in sandstone", Geophysics, 54, 82-89.
•Goodway, B., et al. (1997). Improved AVO Fluid Detection And Lithology Discrimination Using Lamé Petrophysical Parameters;"λρ", μρ, λμ Fluid Stack", From P And S Inversions. 1997 SEG Annual Meeting.
•Hoffe, B. H., et al. (2008). "AVO interpretation in LMR space: A primer", CSEG, Expanded Abstracts.
•Mavko, G., Mukerji, T., and Dvorkin, J. (1998). The rock physics handbook: tools for seismic analysis in porous media. Cambridge University Press.
•Mavko, G., et al. (2009). The rock physics handbook: Tools for seismic analysis of porous media, Cambridge University Press.
•Mur, A. J., (2008), Experimental Rock Physics and Applied Geophysical Models for Long-Term Monitoring of Carbon Dioxide Injected Reservoirs, Ph.D. Thesis, University of Pittsburgh, 223 pp.
•Prasad, M. and R. Meissner (1992). "Attenuation mechanisms in sands: Laboratory versus theoretical (Biot) data." Geophysics 57(5): 710-719.
•Shapiro, S. A., and Kaselow, A., (2005), "Porosity and elastic anisotropy of rocks under tectonic stress and pore-pressure changes", Geophysics 70(5):N27-N38.
•Shapiro, S. A., Becker, K., and Stanchits, S., (2005), "Elastic anisotropy of porous and fractured rocks under stress", Extended Abstracts SEG Annual Meeting.
•Winkler, K. W. (1983). "Frequency dependent ultrasonic properties of high-porosity sandstones." Journal of Geophysical Research: Solid Earth 88(B11): 9493-94Winkler, K. W. and W. F. Murphy III (1995). "Acoustic velocity and attenuation in porous rocks." AGU Reference Shelf 3: 20-34.
•Zimmerman, R. W., Somerton, W. H., and King M. S., (1986), "Compressibility of porous rocks", Journal of Geophysical Research, 91, 12765-12777.

•Acknowledgements
This research was conducted with support from the National Energy Technology Laboratory of the United States Department of Energy.